Ultrastructure and immuno-cytochemistry of BHK-21 cells infected with a modified Bucyrus strain of equine arteritis virus

R. Wada, Y. Fukunaga, T. Kondo, and T. Kanemaru

Epizootic Research Station, Equine Research Institute, The Japan Racing Association,
Tochigi, Japan

Summary. Morphogenesis of a modified Bucyrus strain of equine arteritis virus (EAV) in BHK-21 cells was studied. Bacillary tubules were first detected in the cytoplasm 8 h after infection, and mature virions 79 to 122 nm in diameter, 101 nm on average, were mostly observed in the cisternae of the rough endoplasmic reticulum (RER) at 12 h or later. They had isometrical cores and morphological subunits in the outer layer. Budding occurred from the RER and the outer nuclear membrane, but not from the cell surface. Structural linkage was detected between the tubule and the virus core. Aberrant strands were occasionally demonstrated within the nucleus 12 h after infection, and immunofluorescence and immunogold labeling revealed viral antigen also in the nucleus.

Introduction

Equine arteritis virus (EAV) has been classified into the *Togaviridae* family [22] on the basis of the virion size and morphology [23]. Recently, however, the completely sequenced EAV genome revealed that the virus is of the coronavirus superfamily [7].

The EAV virion was shown to be a spherical particle approximately 60 nm in diameter, consisting of an icosahedral core of 35 nm in diameter surruonded by an envelope [1, 9, 14, 18]. Because of difficulty of treating virions not only in vivo [3, 5, 9] but also in vitro [1], few works have been published on the morphologic characterization of EAV.

In the present study a mutant virus showing higher growth on BHK-21 cells than the parental Bucyrus strain of EAV [11] was examined for the fine structure, its morphogenesis and intracellular localization of viral antigen.

Materials and methods

Cell culture and virus

Confluent monolayers of BHK-21 cells grown in 25 cm² plastic dishes were rinsed with Eagle's minimum essential medium (Eagle's MEM) and they were infected with a mutant virus, the

modified Bucyrus (mB) strain of EAV [19], at a multiplicity of infection of 10. After incubation at 37 °C for 1 h, the infected cultures were rinsed with Eagle's MEM and then received 5 ml of Eagle's MEM with 10% fetal calf serum (maintenance medium). At 4 to 48 h of incubation at 37 °C, samples were taken, and stored at –70 °C for the determination of virus yield and fixed for transmission electron microscopy (TEM). The virus titer was determind by plaque assay, as described by Fukunaga et al. [12].

Indirect immunofluorescence

Monolayer cultures of BHK-21 cells grown on coverslips in perti dishes were washed twice with 0.01 M phosphate-buffered saline (PBS), dried and fixed with aceton at –20 °C for 10 min. They were treated with mouse monoclonal antibody mB1A3 specific for structural protein of EAV [17], which was used as undiluted hybridoma supernatant. After washing 5 times with PBS, the cultures were stained with fluorescent isothiocyanate conjugated goat γ-globulin to mouse γ-globulin at 37 °C for 60 min. After washing with PBS and mouting in SlowFade (Molecular Probes, Inc., OR, USA), the stained samples were examined under the fluorescent microscope.

Transmission electron microscopy

Infected cells were washed twice with 0.05 M sodium cacodylate buffer (pH 7.4), and fixed at 4 °C for 1 h in 2% glutaraldehyde and 0.05 M $CaCl_2$ in the same buffer. Samples were then washed twice in the buffer solution, and postfixed at 4 °C for 30 min in the buffer with 1% osmium tetroxide. Cells were then removed from the plastics using a rubber policeman, pelleted by centrifugation at 12 000 rpm for 5 min, embedded in 1% noble agar, dehydrated in an ascending ethanol series, and embedded in Poly/Bed 812 (Polyscience Inc., PA, USA). Ultrathin sections were made and stained with uranyl acetate (2%, w/v) and Reynold's lead citrate. They were examined using a Hitachi H-7100 electron microscope at 75 kV.

    For immunogold labeling sections were mounted on a 200-mesh nickel grid, which were dipped in PBS containing 0.5% bovine serum albumin for 5 min, and then incubated with monoclonal antibody mB1A3 at room temperature for 60 min. After washing in PBS, the grid was incubated with goat antibody to mouse IgG, which was labeled with 5 nm gold particles (Biocell Co., U.K.) at room temperature for 60 min. After washing in PBS and rinsing in distilled water, the grid was counterstained with uranyl acetate and Reynold's lead citrate.

Results

Growth kinetics of the mB strain of EAV in BHK-21 cells

Viral antigen was first detectable at 8 h after infection and the growth reached a peak at 14 h (Fig. 1). Virus antigen first appeared as fine granules in the cytoplasm of a few cells. Specific fluorescence significantly increased 10 to 12 h after infection in the perinuclear region of the infected cells (Fig. 2a) as well as within the nuclei at 12 h or later (Fig. 2b). Later, the distribution of viral antigen became more generalized within the cytoplasm, although there was some aggregations within the nuclei. No virus-specific fluorescence was seen in uninfected cells and those treated with normal mouse serum and without monoclonal antibody mB1A3.
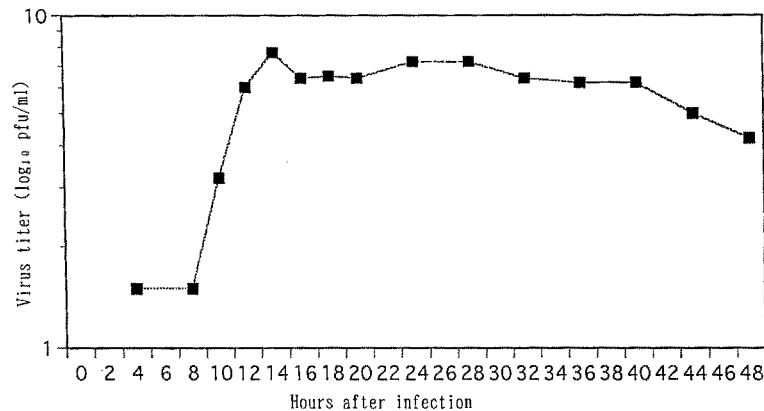
Fig. 1. Titers of the mB strain of EAV on adherent BHK-21 cells at intervals after infection

Morphogenesis of the mB strain of EAV in BHK-21 cells

At 4 to 6 h after virus infection, the cells did not show any morphological changes. At 8 to 10 h an accumulation of ribosomes was shown and a few aberrant strands and short bacillary or tubular branching structures appeared in the cytoplasm. The tubules increased in number thereafter, especially in the vicinity of the nucleus (Fig. 3a). They were more than 200 nm long and on average 42 nm in width, ranging 32 to 52 nm. Aberrant strands were observed frequently in the nucleus at 12 h or later after infection (Fig. 4c).

Virus particles first appeared at 12 h after infection in the cisternae of the rough endoplasmic reticulum (RER) as well as in the perinuclear space. At 14 h virions increased in number in a larger number of cells (Fig. 3a). They were usually spherical or oval 79 to 122 nm, 101 nm average (n=48), in diameter, with isometrical cores 37.8 nm in diameter(n=35). The core had electron-lucent outer layer and dense center with uniformly high opacity (Fig. 3b) or electron lucency (Figs. 3c, e).
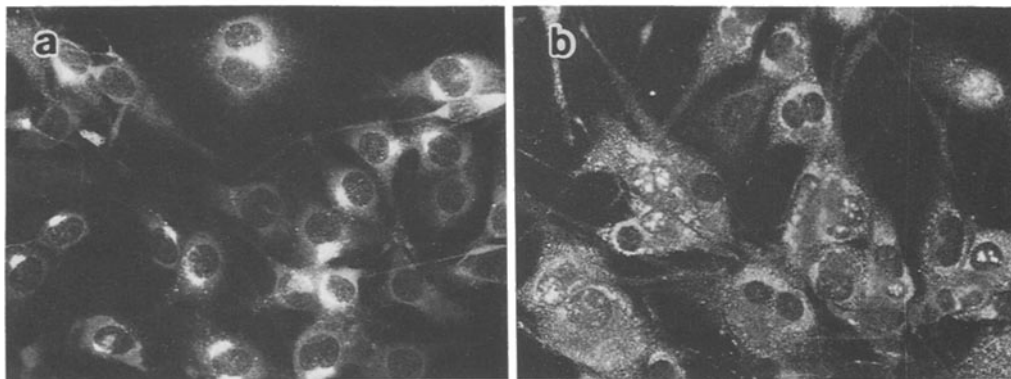

Fig. 2. Specific EAV antigen in the perinuclear area of infected BHK-21 cells at 12 h after infection (**a**) and that distributed in the whole cells at 24 h after infection (**b**) immunofluorescence
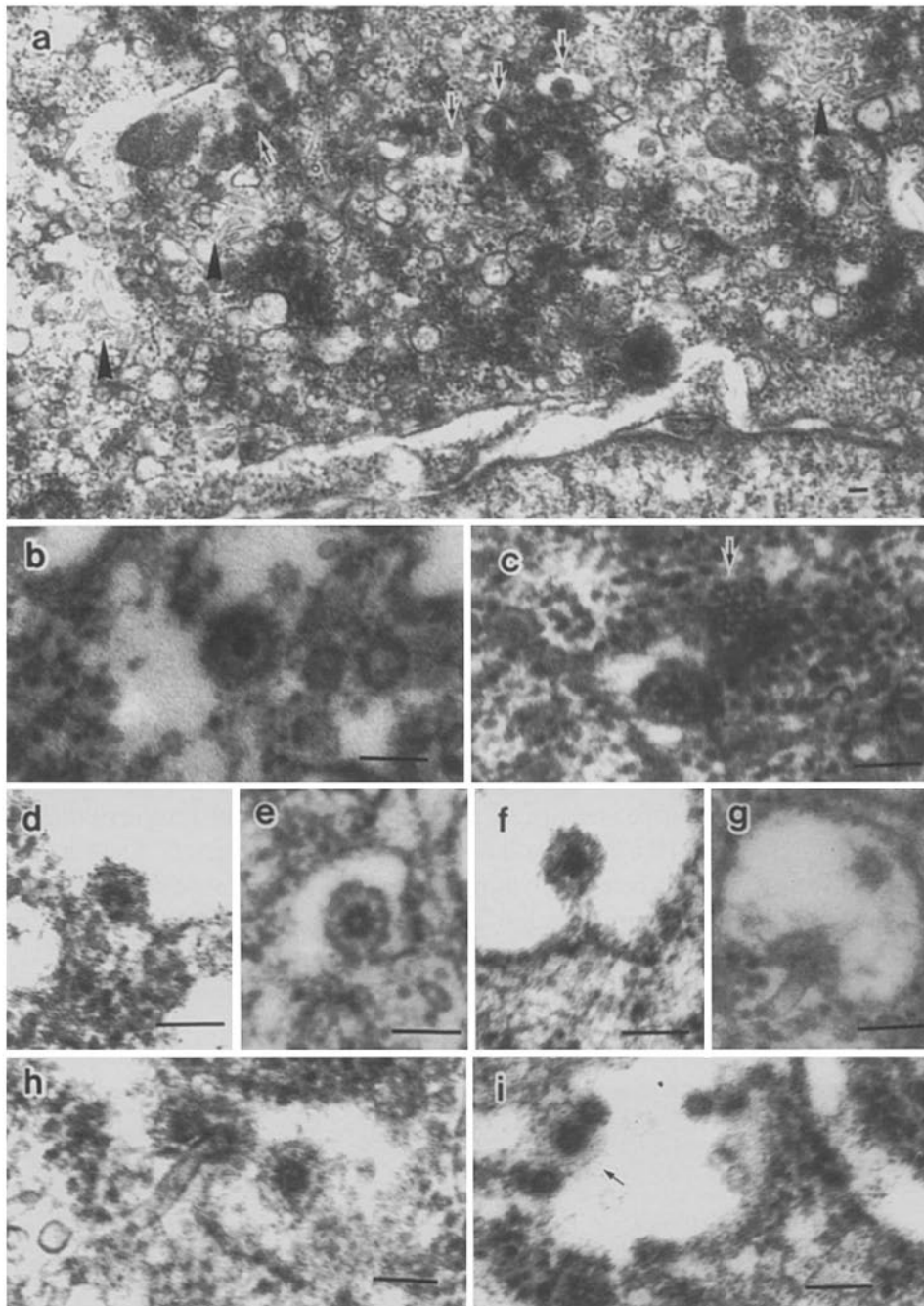
Fig. 3. Electronmicrographs of the mB strain of EAV in BHK-21 cells at 14 h after infection. Bars: 100 nm. **a** Virus particles (arrows) in the RER and numerous tubules (arrowheads) in the cytoplasm. **b** A virion with envelope and projections. **c** Two virions in the RER cisterna. One of them looks like a bunch of grapes (arrow). **d, e, f** Various stages of viral budding into the RER. **g, h** Maturing process showing morphological linkage between the tubule and the virion core. **i** Small particles in a cytoplasmic vesicle. Some of them have an electron-lucent outer layer (arrow)

Through cross-sections of the outer layer of the virion, a grape-like structure seemed to be subunits 13 to 20 nm in diameter around the core (Fig. 3c). Some virions had an envelope with tiny surface projections (Fig. 3b).

Budding of the virus was occasionally observed at the cytoplasmic membrane (Figs. 3d–f). In some budding particles a structural linkage between the tubules and cores of the maturing virions was demonstrated (Fig. 3g, h). On the other hand, other small sized particles about 40 nm in diameter, seemingly in a process maturation, were sometimes observed in the cytoplasmic vesicles (Fig. 3i). Some of them had a very electron-lucent outer layer. Maturation by budding across the cellular membrane could not be found.

Tubules (Fig. 4a) and virus core (Fig. 4b) in the cytoplasm as well as strands (Fig. 4c) in the nucleus were labeled with immunogold staining.

Discussion

EAV has been reported to be morphologically similar to arboviruses [1, 2, 14, 15] and classified into the *Togaviridae* family [10, 13, 22] while morphogenesis of EAV remains unclear. Recently, however, den Boon et al. [7] reported that EAV is evolutionarily related to the coronavirus superfamily. A new virus family, the *Arteriviridae*, which includes the lactate dehydrogenase-elevating virus, lelystad virus and simian hemorrhagic fever virus, has been proposed by Plagemann et al. [20].

EAV are 60 nm in diameter with 12–15 nm ring-like subunits on the surface, having a double membrane structure in an electron-dense core 25 to 35 nm in diameter and possessing an electron-lucent outer envelope [9, 10, 13–15, 18]. Ring-like subunits may exist in the envelope [13, 15]. They also have tiny spikes on their surface [14, 15, 18]. Those structural characteristics were commonly revealed in both purified virus samples [13, 14, 18] and sections [1, 9, 14, 18].

In the present study the mature virions of the mB strain of EAV were 79 to 122 nm in diameter, 101 nm on average, being significantly larger than those reported before. The outline of the mature virions in the RER cisternae was always indefinite, and some of them had distinct surface projections like coronavirus. The mature virions appeared to have subunits in the electron- lucent outer layer. Each subunit was spherical 13 to 20 nm in diameter. These findings suggested that the ring-like subunits were viral capsid components produced inside of the envelope at the budding sites.

Other small sized particles with an approximate diameter of 45 nm were sometimes observed in the cytoplasmic vesicles. They were similar to the typical EAV particles with a thin outer layer around the core [1, 9]. There might be possibilities that: (1) the virus cores broke through a damaged endoplasmic membrane into the vesicles; (2) the outer layer of the small particles was not properly stained; (3) the small particles were incomplete virions without outer subunits. Maturation and budding of the virus appears to occur at RER and perinuclear membrane, but not at the cell membrane.
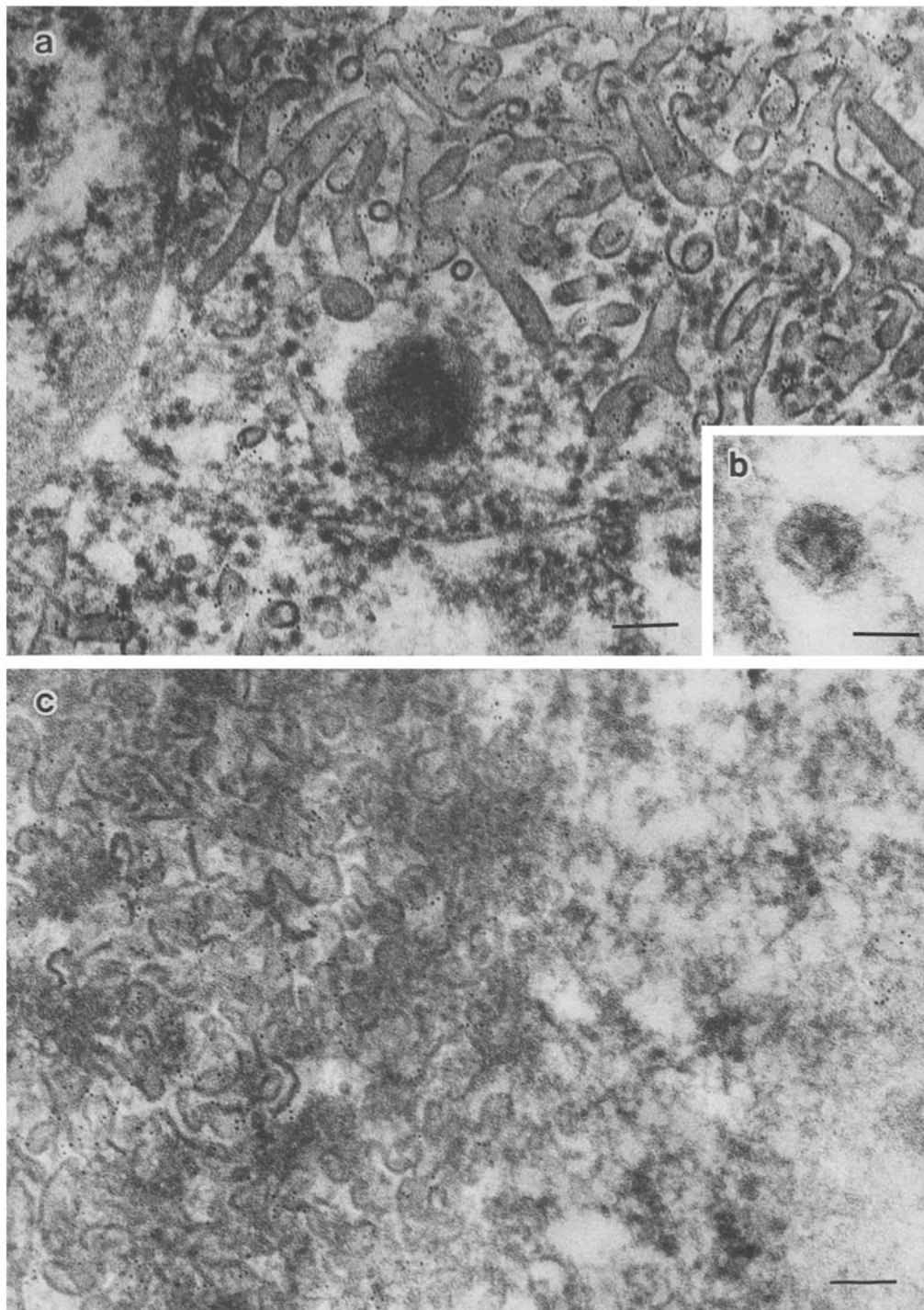
Fig. 4. Tubules (**a**) and a virion (**b**) in the cytoplasm of the BHK-21 cells at 12 h, and strands (**c**) in the nucleus at 24 h after infection, labeled with colloidal gold beads. In **b**, the virus core was labeled with gold beads. Electron microscopy with immunogold staining. Bars: 100 nm

A large number of tubules, assumed to be specific structures related with the replication of EAV in vivo [9] and in vitro [2], were observed in BHK-21 cells infected with the mB strain of EAV. In this study, a structural linkage was detected between the tubules and the virus core. These tubules reacted with immunogold-labeled antibody to EAV. Similar tubules have been described also in infections with lactate dehydrogenase-elevating virus [21], mouse hepatitis virus [8] and bluetongue virus [4], while larger number of tubules appeared in infection with the mB strain of EAV.

No ultrastructural or immuno-cytochemical change in the nucleus has been observed previously [2, 6, 16, 18]. In this study, however, EAV-specific ultrastructural and immunofluorescent findings were shown in the nucleus. By immunogold labeling of thin sections, antigen was detectable not only on the cytoplasmic tubules but also on strands in the nucleus. These findings suggested the same viral components were present in different forms in both sites. It could not be determined whether the strands in the nucleus were precursors of tubules or they represented in dead-end stage of the virus wandering in the nucleus, since no morphological transition was observed.

Acknowledgement

References

1. Breese SS, McCollum WH (1970) Electron microscopic characterization of equine arteritis virus. Proc 2nd Int Conf Equine Infectious Diseases: 133–139
2. Breese SS, McCollum WH (1971) Equine arteritis virus: ferritin-tagging and determination of ribonucleic acid core. Arch Ges Virusforschung 35: 290–295
3. Breese SS, McCollum WH (1973) Electron-microscopic studies of tissues of horses infected by equine arteritis virus. Proc 3rd Int Conf Equine Infectious Diseases, pp 273–281
4. Brewer AW, MacLachlan NJ (1994) The pathogenesis of bluetongue virus infection of bovine blood cells in vitro: ultrastructural characterization. Arch Virol 136: 287–298
5. Coignoul FL, Cheville NF (1984) Pathology of maternal genital tract, placenta, and fetus in equine viral arteritis. Vet Pathol 21: 333–340
6. Crawford TB, Davis WC (1970) Fluorescent and electron microscope studies of equine arteritis virus (Abstr.). Fed Proc 29: 286
7. den Boon JA, Snijder EJ, Chirnside ED, de Vries AAF (1991) Equine arteritis virus is not a togavirus but belongs to the coronavirus-like superfamily. J Virol 65: 2910–2920
8. Dubois-Dalcq ME, Doller EW, Haspel MV, Holmes KV (1982) Cell tropism and expression of mouse hepatitis viruses (MHV) in mouse spinal cord cultures. Virology 119: 317–331
9. Estes PC, Cheville NF (1970) The ultrastructure of vascular lesions in equine viral arteritis. Am J Pathol 58: 235–253
10. Francki RIB, Fauquet CM, Knudson DL, Brown F (1991) Classification and Nomenclature of viruses. Fifth Report of the International Committee on Taxonomy of Viruses. Springer, Wien New York, pp 220–222 (Arch Virol [Suppl] 2)
11. Fukunaga Y, McCollum WH (1977) Complement-fixation reaction in equine viral arteritis. Am J Vet Res 38: 2043–2046

12. Fukunaga Y, Imagawa H, Tabuchi E, Akiyama Y (1981) Clinical and virological findings on experimental equine viral arteritis in horses. Bull Equine Res Inst 18: 110–118

13. Horzinek M, Maess J, Laufs R (1971) Studies on the substructure of togaviruses. II. Analysis of equine arteritis, rubella, bovine viral diarrhea, and hog cholera viruses. Arch Ges Virusforschung 33: 306–318

14. Hyllseth B, Magnusson P, Marusyk H (1970) Studies on equine arteritis virus. Proc 2nd Int Conf Equine Infectious Diseases, pp 140–142

15. Hyllseth B (1973) Structural proteins of equine arteritis virus. Arch Ges Virusforschung 40:177–188

16. Inoue T, Yanagawa R, Shinagawa M (1975) Immunofluorescent studies on the multiplication of equine arteritis virus in Vero and E. Derm (NBL-6) cells. Jpn J Vet Sci 37: 596–575

17. Kondo T, Akashi H, Fukunaga Y, Sugita S, Sekiguchi K, Wada R, Kamada M (1995) Production and characterization of monoclonal antibodies against structural proteins of equine arteritis virus. Proc 7th Int Conf Equine Infectious Diseases, pp 21–26

18. Magnusson P, Hyooseth B, Marusyk H (1970) Morphological studies on equine arteritis virus. Arch Ges Virusforschung 30: 105–112

19. McCollum WH (1969) Development of a modified virus strain and vaccine for equine viral arteritis. J Am Vet Med Assoc 115: 318–322

20. Plagemann PGW, Moennig V (1991) Lactate dehydrogenase-elevating virus, equine arteritis virus and simian hemorrhagic fever virus: a new group of positive-strand RNA viruses. Adv Virus Res 41: 99–192

21. Stueckemann JA, Ritzi DM, Holth M, Smith MS, Swart WJ, Cafruny WA, Plagemann PGW (1982) Replication of lactate dehydrogenase-elevating virus in macrophages. 1. Evidence for cytocidal replication. J Gen Virol 59: 245–262

22. Westaway EG, Brinton MA, Gaidamovich SYA, Horzinek MC, Igarashi A, Kaariainen L, Lvov DK, Porterfield JS, Russell PK, Trent DW (1985) Togaviridae. Intervirology 24: 125–139

23. Wildy P (1971) Classification and nomenclature of viruses. First report of the international committee on nomenclature of viruses. Monogr Virol 5: 1–81

Authors' address: Dr. R. Wada, Epizootic Research Station, Equine Research Institute, The Japan Racing Association, 1400-4, Shiba, Kokubunji-machi, Shimotsuga-gun, Tochigi 329-04, Japan.